Journal of Harbin Engineering University
ISSN: 1006-7043

Vol 45 No. 9
September 2024

Proposing an Innovative Radiofrequency Ablation Method for Liver Tumour Treatment: A Computational Study Ablation

Mahmoud Jamalie [a,d],Seyed Mohammad Mahdi Modarres Mosalla [a,c],Hassan Tavakoli [a,b]*,Ahmad Khoncheh [c],Amin Shahverdi [d],Mohammadhossein Kouhpaeenejad [c]

a. Radiation Injuries Research Centre, Baqiyatallah University of Medical Sciences, Tehran, Iran.

b. Department of Physiology and Medical Physics, School of Medicine, Baqiyatallah University of Medical Sciences, Tehran, Iran.

c. School of Medicine, Baqiyatallah University of Medical Sciences, Tehran, Iran.

d. Student Research Committee, Baqiyatallah University of Medical Sciences, Tehran, Iran

Abstract

Introduction: Liver cancer is one of the most prevalent cancers worldwide, claiming over thousands of lives annually. Various treatment methods have been employed, but each suffers from several shortcomings that challenge their therapeutic efficacy. Nonetheless, Radiofrequency Ablation (RFA) has recently garnered significant attention from medical professionals. Despite its effectiveness, this treatment approach presents a critical challenge: the unintended penetration of heat into healthy liver tissues, particularly in the areas surrounding the tumor.

Objectives: How to add phase change material nanoparticles in the marginal areas and healthy liver tissue to prevent unwanted temperature increases. For this purpose, a model of healthy tissues, the marginal area, and the liver tumour were first simulated.

Methods: A radiofrequency antenna, designed and simulated as a probe, was utilized as a heat source in the tumor region. By defining the appropriate parameters, the distribution of heat energy within each area was determined as an electromagnetic and heat transfer problem for the software. The finite element method was employed to solve the problem in the presence and absence of nanoparticles. The results were then presented in the form of thermogram graphs.

Results: The findings revealed that the heat generated within the tumour effectively destroyed the cancer cells, indicating a successful RFA process. However, the obtained thermogram demonstrated that thermal energy inevitably penetrated the healthy tissue, particularly in the marginal area, causing an increase in temperature. Conversely, examining the heat distribution pattern in the marginal and healthy tissues showed that using paraffin significantly reduced the unwanted temperature increase. Even the temperature decreased to its natural value in areas distal to the tumour centre.

Conclusions: In conclusion, nanoparticles, appear to effectively preserve healthy liver tissues while enhancing the efficiency of liver tumour treatment during RFA. This, in turn, improves the therapeutic effect of RFA in liver tumour management.

Keywords: Cancer, hyperthermia, cancer cells, tumour ablation, finite element method.

1. Introduction

In the field of hyperthermia, there are differences and contradictions among studies regarding the level of temperature, the duration of heating, and the number of heating sessions in this method, and there is no unified protocol in this regard, which has led to difficulties in evaluating and comparing different hyperthermia methods (3). Magnetic nanostructures used for hyperthermia can be paramagnetic or ferromagnetic, exhibiting magnetic properties without the presence of a field, and magnetic nanoparticles such as iron oxides have magnetic spins all aligned; a variable magnetic field can provide the necessary

Corresponding author, Email address: tavakoli@bmsu.ac.ir

energy to misalign magnetic spins in the nanostructured material. This magnetic energy, when released, can be converted into thermal energy because to realign magnetic spins, this energy can also physically rotate nanostructures, which the resulting thermal energy is used to generate heat within the cell (4). Also, the friction generated by the rotation of magnetic nanostructures in a fluid with high viscosity and density until reaching a physical equilibrium state can create heat. Therefore, the method of generating heat by a magnetic fluid for cancer treatment involves directly injecting a magnetic fluid carrier containing magnetic nanostructures into cancerous tumour, when the patient is placed in a variable magnetic field with frequencies close to radio signals, in which case magnetic nanoparticles generate heat and destroy the cancerous tumour. Also, methods using laser, microwave, or ultrasound to generate heat in tissue are used (5). One of the magnetic nanostructures that has received attention in recent years is cobalt ferrite. Its suitable physical, chemical, and magnetic properties, as well as important features such as high permeability, low magnetic losses, shape change due to magnetization, as well as mechanical hardness and high chemical stability, are among the characteristics of cobalt ferrite (CoFe2O4) (6). Studies on cell cultures outside the body as well as results obtained from induced cells inside the body have provided convincing justification for the clinical application of hyperthermia.

Results from clinical studies have provided new insights into the mechanisms of hyperthermia and cancer treatment (7). One hypothesis is that hypoxia, which is caused by an increase in the pH of the tumour area, creates resistance in tumour areas sooner than expected due to their high sensitivity to hypoxia (7). In a study by Dewey et al. (8), it was reported that hyperthermia treatment has two main advantages in cancer treatment. Firstly, in the cell cycle, the S phase usually shows resistance to radiation. However, this phase is most susceptible to heat. Therefore, a combined approach of radiation therapy with hyperthermia is more effective. Another advantage is that hyperthermia is necessary to kill cancer cells that have become hypoxic due to radiation therapy. However, clinical application of these methods has its challenges, including determining the optimal temperature and time for using this combined approach, and another issue in local hyperthermia is damage to adjacent tissues, which always needs to be addressed. Many studies have been conducted in the field of modelling cancer tissue hyperthermia from a heat transfer perspective. In most past studies, it was assumed that the distribution of nanoparticles inside the tumour is uniform. Attar et al. (9) reported on the investigation of tissue temperature distribution under magnetic fluid treatment, assuming a non-uniform distribution of nanoparticles inside the tumour, demonstrating that the tissue temperature profile is observable. Also, the thermal effect of magnetic fluid in the liver tissue of a pig was experimentally examined. In that study, the Penn bioheat transfer equation was solved for a non-uniform distribution of nanoparticles inside cancer tissue exposed to an AC magnetic field. The results clearly showed the importance of nanoparticle distribution in tissue. Even a slight tendency of nanoparticle concentration from cancerous tissue towards healthy tissue can significantly increase the likelihood of damage to healthy tissue. Another hyperthermia method that modelling can help improve is RFA method.

Another type of hyperthermia method that has been modelled is laser therapy. Laser therapy can be performed alone or by delivering nanotubes or nanoparticles into the tumour to enhance the laser effect, for which models have been developed for both cases. He et al. (10) worked on modelling laser therapy by considering changes in blood flow rate and distribution of partial oxygen pressure (PO2). Their study aimed to investigate changes in blood flow rate and distribution of partial oxygen pressure in human tumour during laser therapy by simultaneously solving two numerical models during laser therapy. A two-dimensional thermal model of the human chest with a tumour inside it was prepared. Blood circulation inside the chest was modelled by a one-dimensional nonlinear fluid flow equation. PO2 distribution inside the capillaries, tumour vessels, and surrounding tissue was provided by the Krogh's analysis model. Finally, changes in the average temperature of a tumour, blood flow, and PO2 during heating with lasers were calculated by simultaneously solving models of blood circulation, finite heat elements, and oxygen transport. Rossi et al. (10) modelled laser therapy using nanotubes with the help of COMSOL software in 2012. Photothermal therapy with gold nanorods (GNRs) is a new minimally invasive treatment method for cancer tissues. For designing appropriate settings and conditions, it is important to investigate the thermal effects occurring around nano particles (in a nano-sized model). In this study, this investigation was conducted

for the vicinity and inside cancerous tissue (in a micro-sized model). A two-dimensional temperature-dependent model of this photo-thermal interaction was designed. A cross-sectional area of gold nanotubes, which was considered as the absorber, was used to calculate the optical absorption of the gold nanotubes. Subsequently, the bioheat transfer equation was applied to describe the photothermal effect between the gold nanotubes and the environment. The results, after processing, can assist in calculating the safe and probable temperature range and treatment duration for the complete destruction of the tumour. Hatami et al. (11) employed cobalt graphene nanoparticles for hyperthermia and MRI diagnosis. In this study, composites were synthesized chemically. Graphene oxide was considered as the base material, and cobalt nanoparticles with a size of 15 nanometers were deposited on graphene sheets, showing that the concentration of cobalt in the nanocomposite is approximately 80 percent. Additionally, the toxicity of the graphene/cobalt nanocomposite was investigated.

2. Objectives

Recent studies indicate that liver cancer is among the most common cancers globally. Traditional treatments, including surgery, radiotherapy, and chemotherapy, often face considerable difficulties. These include the risk of infections, high costs, low success rates, the likelihood of cancer spreading to other organs such as the intestine and gallbladder, and extended recovery times. In light of these significant issues, RFA has gained attention as a potential treatment option for liver cancer. However, a key concern with this method is its ability to target the cancerous tissue while safeguarding the healthy liver tissue, particularly hepatocytes, from excessive and unintended temperature rises. To tackle this major challenge, this study explores how phase change materials (PCMs) can prevent temperature increase in healthy tissue during RFA, this point is the novelty of this study. To gain a deeper understanding of how these materials function, the problem was modelled using COMSOL Multiphysics simulation software, and the solution was derived through numerical analysis.

3. Methods

The liver tumour region was modeled as a sphere with a diameter of 30 mm, while radius of the liver tissue is 140 mm. Previous research (28,29) affirmed that the chosen size for the liver region was sufficient. Two RF probes, one featuring a positive electrode and the other a negative electrode, each with a r= 1 cm and an active length of 30 mm, were vertically placed through the tumour at a specified distance from the tumour region. Both probes were introduced through the tumour, with a 1 cm gap between them. In Figure 1, the 3D model of the liver and tumour is illustrated, including the geometric depiction of the gap. PCMs are introduced into cancer cells. The model simulation is conducted in an axisymmetric manner, acknowledging axial symmetry within the thermal domain. Following certain assumptions and simplifications outlined in subsequent sections, the asymmetric model is employed to examine the proposed method in this investigation.

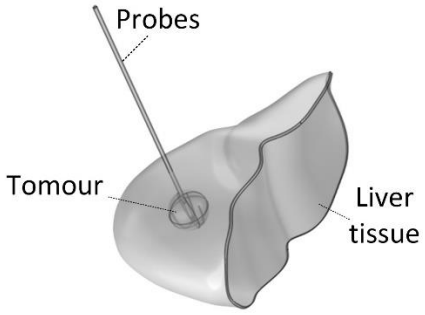

(a)

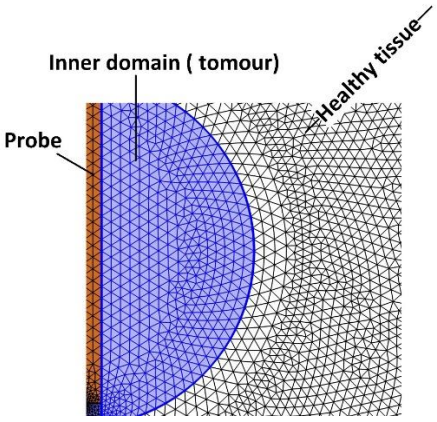

(b)

Fig. 1 3D (a) and axisymmetric (b) models used in the RFA cancer ablation method proposed in this study.

The complexity of RFA lies in the combined effects of electrical potential distribution, temperature

distribution, and the formation of thermal coagulation within tissues. RFA involves an electrical current with a frequency ranging from 350 to 500 kHz. As a result, the characterization of the electrical potential distribution in RFA can be achieved through the following Equations (28):

$$\nabla.(\sigma.\nabla\phi) = 0 \quad (1)$$

where σ and ϕ represents the electrical conductivity and potential of the tissue, respectively. Equations (3) and (4) are temperature variation in tissue and Arrhenius damage equations and are expressed as (28):

$$\rho c\frac{\partial T}{\partial t} = \nabla.(\mathrm{k}\nabla T) + \omega\rho_b c_b(T_b - T) + \sigma|\nabla\phi|^2 \quad (2)$$

$$\frac{d\Omega}{dt} = \frac{A}{e^{(\Delta E/RT)}} \quad (3)$$

where ρ, c, and T are tissue density, tissue specific heat, and tissue temperature. Superscript b denotes arterial. The symbol Ω is utilized as a parameter to measure the degree of thermal coagulation within the tissue. A denotes the frequency factor, E represents the activation energy arising from an irreversible thermal energy damage reaction, and R is the universal gas constant. The specific values for the constant parameters mentioned in Equations (1-3) and the material properties assigned to the tissue are derived from the findings presented in (28,30). In the course of RFA, the temperature in the vicinity of the RF probes may rise above the boiling point of water. Consequently, the water within the tissue undergoes vaporization, impacting the heat transfer dynamics within the tissue. Terms of ρc and k are dependent on T_u (upper vapourisation temperature of blood) and T_L (lower vapourisation temperature of blood) (28). The assumption is made that the electrical conductivity ($\delta(T)$) increases with temperature. Coagulation-dependent blood perfusion and impedance-controlled ablation are estimated for the model simulated in this study based on the results of the work of Yap et al. (28). The electrical conductivity model used in this study is based on the reference (29).

A heat capacity model is employed to analyse the impact of substances undergoing phase change within healthy tissues. C_{eq}, k_{eq} shows the equivalent heat capacity and thermal conductivity used for PCM in calculations based on the reference (29). It is essential to compute the thermal equivalent properties for healthy tissues following the injection of PCMs due to the alterations in the thermal characteristics of PCMs (26). α represents the volume fraction of PCMs within the healthy tissue region. The study utilises the equivalent heat capacity method (26) to examine the impact of PCMs in healthy tissues.

Table 1 shows the properties of liver and liver tumour tissues and PCMs. Main assumptions are based on PCMs that all PCMs consist of uniformly dispersed spherical particles with identical radius within the region of healthy tissue (26). The transition from solid to liquid phase for PCMs occurs within the temperature range mentioned in Table 1. There is no alteration in volume during the phase change process of PCMs (26).

Table 1 Material properties of tissues and PCM used in this study.

	Parameter	Value
Liver	ρ	$1060\ {}^{\mathrm{kg}}/_{\mathrm{m}^3}$
	k	$0.53\ {}^{\mathrm{W}}/_{\mathrm{mK}}$
	c	$3500\ {}^{\mathrm{J}}/_{\mathrm{kg\,K}}$
	σ	$0.35\ {}^{\mathrm{S}}/_{\mathrm{m}}$
	A	$739 * 10^{37}\ {}^{1}/_{\mathrm{s}}$
Tissue	ρ	$1060\ {}^{\mathrm{kg}}/_{\mathrm{m}^3}$
	k	$0.53\ {}^{\mathrm{W}}/_{\mathrm{mK}}$
	c	$3500\ {}^{\mathrm{J}}/_{\mathrm{kg\,K}}$
	σ	$0.57\ {}^{\mathrm{S}}/_{\mathrm{m}}$
	ω_b	$0.002\ {}^{1}/_{\mathrm{s}}$

To conduct mesh convergence analysis, the model is solved with varying numbers of elements as shown in Fig. 2. Given the significance of the temperature at the tumour center, this parameter is investigated across different element numbers. The simulation is carried out, assuming for the initial t=100s, and the temperature is recorded at the tumour's central point. The number of 22745 elements is identified as the best model.

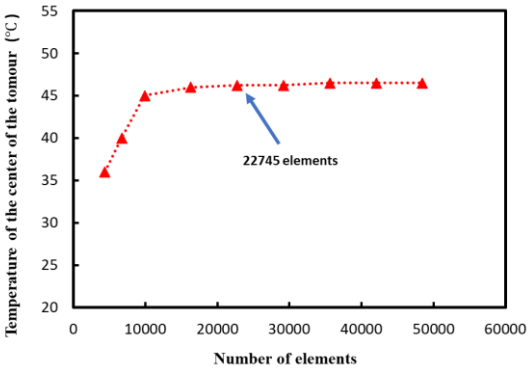

Fig. 2 Mesh convergence analysis.

4. Results

For the validation model, a tissue without cancerous liver tumour is considered. The temperature at the center of the tissue is compared with that of the reliable reference (28). The physics incorporated into the dual-probe bipolar RFA model developed in this study underwent validation by comparing with the results of (28) as shown in Fig. 3. The RF probes' active length was set at a constant 30 mm. Initial tissue temperature and outer boundary were established at 18 °C. Further properties are based on the data given in Table 1.

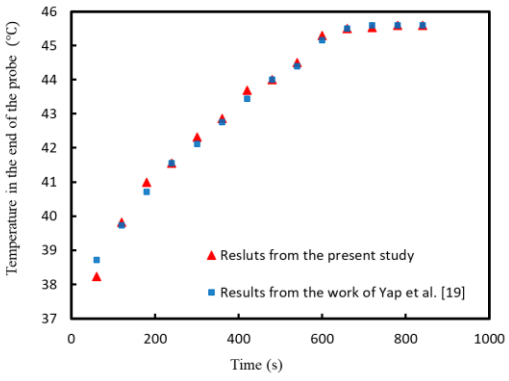

Fig. 3 Model validation by comparing the temperature in the center of the liver tissue of the model with that of the Yap et al. (28).

In this research, PCMs have been utilized to control the temperature of healthy cells surrounding cancerous tissue during the elimination of cancer cells. By calculating the temperature contour energy equations in the cancerous tumour and its surrounding environment, evidence of temperature control using phase-changing agents has been obtained. In Fig. 4, the contour of electric potential around the probe is shown, the electric potential leads to temperature increase through the cancerous tissue as well as healthy tissue.

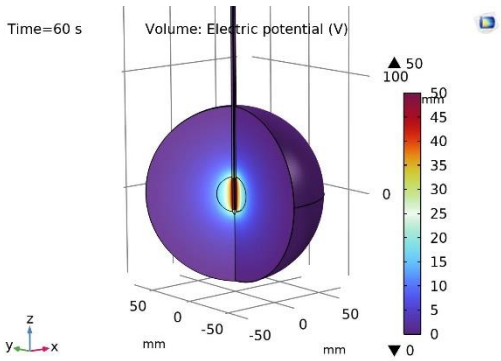

Fig. 4 Electric potential around the probe.

Fig. 5 shows the contour of the temperature distribution for different times from *t*=0 min to *t*=10 min.

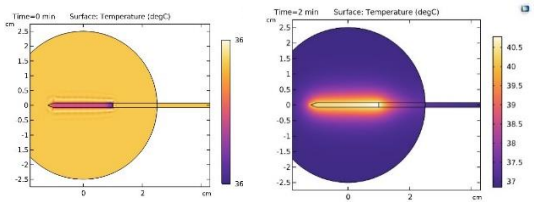

t=0 min *t*=2 min

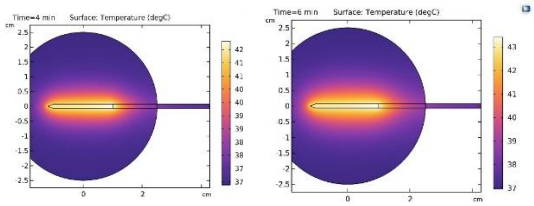

t=4 min *t*=6 min

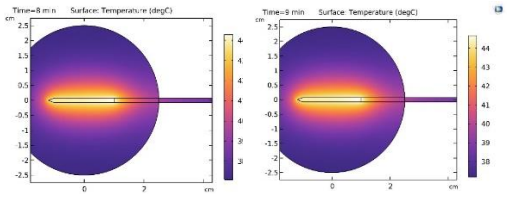

t=8 min *t*=9 min

Fig. 5 Temperature distribution in cancerous liver tumour at *t*=0-9 min.

By using PCMs around cancerous tumour, the temperature increase undergoes changes compared with the model without PCMs. In Fig. 6, the temperature on the axis located at the center of tumour is shown for the model with and without PCMs at four different times (*t*= 8,9,10,11 min).

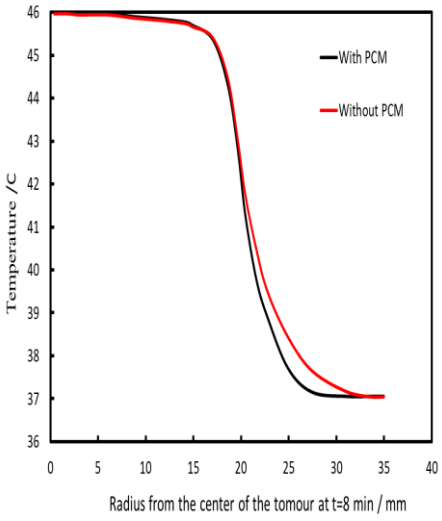

t=8 min

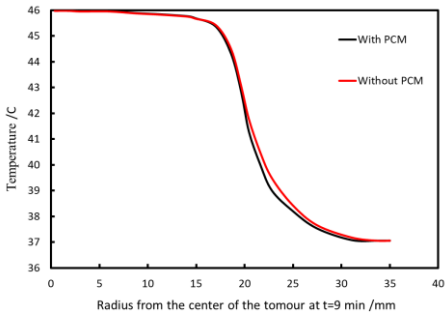

t=9 min

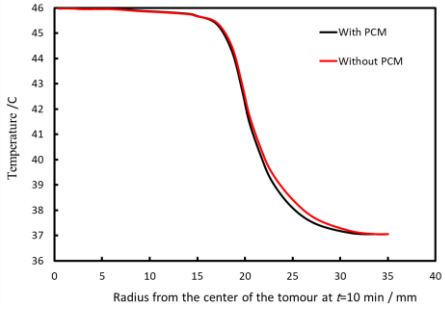

t=10 min

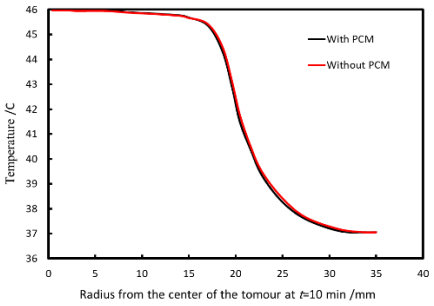

t=11 min

Fig. 6 Temperature in different radius from the center of the tumour from t=8 min to *t*=11 min.

Fig. 6 shows the effect of using PCM leads to temperature decrease in healthy tissue at *r*=15-35 mm. The maximum temperature difference occurs at *t*=9 min, after this time the temperature difference between two models with and without PCMs, decreases, and the temperature diagrams of the two models converge closely. At *t*=8, 10 and 11 min, the temperature of the two models is closer than the model at *t*=9 min, results show that PCM after *t*=9 min are completely liquefied and cannot maintain the temperature anymore, it means that the effect of PCM after *t*=9 min are diminishing. As shown in Fig. 6, temperature diagrams almost coincide at *t*=11min.

5. Discussion

In conclusion, the study conducted FEM on an axymmetric model. The results demonstrate that an appropriate frequency and probe placement can elevate the temperature of cancerous tumour, leading to their destruction. This research introduces a RFA method for destroying cancerous liver tumour while safeguarding healthy cells by regulating the temperature of the area containing healthy cells through the injection of PCM nanoparticles. The investigation emphasizes a significant reduction in temperature for healthy tissues surrounding a liver tumour, maintaining it within a controllable temperature range using PCMs. This decrease plays a crucial role in minimizing tissue damage during the release of heat in cancerous liver tumour due to the RFA probe. Additionally, the influence of PCMs on tissue temperature distribution shows an increase over time, specifically until *t*=9 minutes, before and after this time the temperature difference is less.

References

[1] Andreozzi A, Brunese L, Iasiello M, Tucci C, Vanoli GP. Modeling Heat Transfer in Tumors: A Review of

Thermal Therapies. Vol. 47, Annals of Biomedical Engineering. 2019.

[2] Darvishi V, Navidbakhsh M, Amanpour S. Heat and mass transfer in the hyperthermia cancer treatment by magnetic nanoparticles. Heat Mass Transf und Stoffuebertragung. 2022;58(6).

[3] Cheung AY, Neyzari A. Deep local hyperthermia for cancer therapy: External electromagnetic and ultrasound techniques. Cancer Res. 1984;44(10 SUPPL.).

[4] Shields JA, Shields CL, Scartozzi R. Survey of 1264 patients with orbital tumors and simulating lesions: The 2002 Montgomery Lecture, part 1. Ophthalmology. 2004;111(5).

[5] Gottlieb CF, Seibert GB, Block NL. Interaction of irradiation and microwave-induced hyperthermia in the Dunning R3327G prostatic adenocarcinoma model. Radiology. 1988;169(1).

[6] Manova E, Kunev B, Paneva D, Mitov I, Petrov L, Estournès C, et al. Mechano-synthesis, characterization, and magnetic properties of nanoparticles of cobalt ferrite, CoFe2O4. Chem Mater. 2004;16(26).

[7] Kaur P, Hurwitz MD, Krishnan S, Asea A. Combined hyperthermia and radiotherapy for the treatment of cancer. Vol. 3, Cancers. 2011.

[8] Dewey WC, Hopwood LE, Sapareto SA, Gerweck LE. Cellular responses to combinations of hyperthermia and radiation. Vol. 123, Radiology. 1977.

[9] Attar MM, Haghpanahi M, Amanpour S, Mohaqeq M. Analysis of bioheat transfer equation for hyperthermia cancer treatment. J Mech Sci Technol. 2014;28(2).

[10] Rossi F, Ratto F, Pini R. Laser Activated Gold Nanorods for the Photothermal Treatment of Cancer. COMSOL Conf. 2012;

[11] Hatamie S, Ahadian MM, Ghiass MA, Iraji zad A, Saber R, Parseh B, et al. Graphene/cobalt nanocarrier for hyperthermia therapy and MRI diagnosis. Colloids Surfaces B Biointerfaces. 2016;146.

[12] Beik J, Abed Z, Ghoreishi FS, Hosseini-Nami S, Mehrzadi S, Shakeri-Zadeh A, et al. Nanotechnology in hyperthermia cancer therapy: From fundamental principles to advanced applications. Vol. 235, Journal of Controlled Release. 2016.

[13] Bao J, Tu H, Li J, Li Y, Yu S, Gao J, et al. Applications of phase change materials in smart drug delivery for cancer treatment. Vol. 10, Frontiers in Bioengineering and Biotechnology. 2022.

[14] Hu X, Li H, Li R, Qiang S, Chen M, Shi S, et al. A Phase-Change Mediated Intelligent Nanoplatform for Chemo/Photothermal/Photodynamic Therapy of Cancer. Adv Healthc Mater. 2023;12(5).

[15] Taheri AA, Taghilou M. Towards a uncertainty analysis in thermal protection using phase-change micro/nano particles during hyperthermia. Int J Eng Trans A Basics. 2021;34(1).

[16] Taheri AA, Talati F. FDM-based 2D Numerical Study of Hyperthermia Cancer Treatment by Micro/Nano-Phase-Change Materials. Iran J Sci Technol - Trans Mech Eng. 2020;44(4).

[17] Li J, Liu Y, Li X, Liang G, Ruan C, Cai K. ROS self-generation and hypoxia self-enhanced biodegradable magnetic nanotheranostics for targeted tumor therapy. Nanoscale Horizons. 2020;5(2).

[18] Lv YG, Deng ZS, Liu J. 3-D Numerical Study on the Induced Heating Effects of Embedded Micro/Nanoparticles on Human Body Subject to External Medical Electromagnetic Field. IEEE Trans Nanobioscience. 2005;4(4).

[19] Liu KC, Chen TM. Comparative study of heat transfer and thermal damage assessment models for hyperthermia treatment. J Therm Biol. 2021;98.

[20] Moradpoor R, Aledavood SA, Rajabi O, Chamani JK, Sazgarnia A. Enhancement of cisplatin efficacy by gold nanoparticles or microwave hyperthermia? An in vitro study on a melanoma cell line. Int J Cancer Manag. 2017;10(1).

[21] Lv Y, Zou Y, Yang L. Theoretical model for thermal protection by microencapsulated phase change micro/nanoparticles during hyperthermia. Heat Mass Transf und Stoffuebertragung. 2012;48(4).

[22] 22. Comanescu C. Magnetic Nanoparticles: Current Advances in Nanomedicine, Drug Delivery and MRI. Vol. 4, Chemistry (Switzerland). 2022.

[23] Tang Y, Jin T, Flesch RCC. Numerical temperature analysis of magnetic hyperthermia considering nanoparticle clustering and blood vessels. IEEE Trans Magn. 2017;53(10).

[24] Tang Y, Chen H, Gao Y. Optimization for magnetic field distribution in ferrite core and its effect on magnetic hyperthermia. Zhongnan Daxue Xuebao (Ziran Kexue Ban)/Journal Cent South Univ (Science Technol. 2023;54(8).

[25] Skumiel A, Musiał J. The use of Gramme coils in a 2-phase system for generation of a high frequency

rotating magnetic field. J Magn Magn Mater. 2022;564.

[26] Tang Y dong, Flesch RCC, Zhang C, Jin T. Numerical analysis of the effect of non-uniformity of the magnetic field produced by a solenoid on temperature distribution during magnetic hyperthermia. J Magn Magn Mater. 2018;449.

[27] Taheri AA, Talati F. Numerical study of induction heating by micro / nano magnetic particles in hyperthermia. J Comput Appl Res Mech Eng. 2020;9(2).

[28] Yap S, Cheong JKK, Foo JJ, Ooi ET, Ooi EH. The effects of the no-touch gap on the no-touch bipolar radiofrequency ablation treatment of liver cancer: A numerical study using a two compartment model. Appl Math Model. 2020;78.

[29] Ooi EH, Lee KW, Yap S, Khattab MA, Liao IY, Ooi ET, et al. The effects of electrical and thermal boundary condition on the simulation of radiofrequency ablation of liver cancer for tumours located near to the liver boundary. Comput Biol Med. 2019;106.

[30] Haemmerich D, Wood BJ. Hepatic radiofrequency ablation at low frequencies preferentially heats tumour tissue. Int J Hyperth. 2006;22(7).

[31] Hall SK, Ooi EH, Payne SJ. Cell death, perfusion and electrical parameters are critical in models of hepatic radiofrequency ablation. Int J Hyperth. 2015;31(5).